

Model Predictive Control of a STATCOM based on a Modular Multilevel Converter in Delta Configuration

Tobias Geyer*, Georgios Darivianakis[†] and Wim van der Merwe[‡]

* ABB Corporate Research, Baden-Dättwil, Switzerland.

[†] Automatic Control Laboratory, ETH Zürich, Switzerland.

[‡] ABB Medium Voltage Drives, Turgi, Switzerland.

Emails: t.geyer@ieee.org, gdarivia@control.ee.ethz.ch, wim.van-der-merwe@ch.abb.com

Keywords

«Converter Control», «Model Predictive Control», «Optimal Control», «Modular Multilevel Converter», «Static Synchronous Compensator (STATCOM)».

Abstract

This paper proposes a model predictive control (MPC) scheme for the single delta bridge cell (SDBC) modular multilevel converter (MMC) when operated as a static synchronous compensator (Statcom). The controller achieves reactive power compensation and current harmonic elimination while maintaining the branch currents and capacitor voltages within their safe operating limits. The MPC scheme manipulates the setpoints of a subsequent pulse width modulator (PWM). The controller is conceptually simple with an easy to devise objective function, a linearized converter model based on first principles, and constraints on the main physical quantities. The underlying optimization problem is a quadratic program (QP), which can be solved efficiently using off-the-shelf solvers. The developed control framework achieves a good performance at steady-state operation and very fast current response during load transients.

1 Introduction

Power quality issues arise in modern medium voltage distribution systems due to the wide-spread use of nonlinear loads such as diode front ends, motor drives, electrical furnaces and welding devices. These nonlinear loads draw reactive power, inject current harmonics and impose phase unbalances onto the distribution system [1]. The single delta bridge cell (SDBC) modular multilevel converter (MMC) has the capability of compensating for reactive power and to inject current harmonics [2]. In addition, it has the capability to operate continuously under unbalanced grid voltages and currents [3].

The series-connection of identical, yet individually controllable module capacitors facilitates the scaling of the output voltage of the MMC [4]. This enables operation at high voltages and high power. Increasing the number of output voltage levels is also instrumental to meet stringent harmonic requirements at the point of common coupling (PCC). Low line current total harmonic distortions (THD) can be achieved even when operating at very low device switching frequencies. This makes the SDBC-MMC topology a suitable choice for high power static synchronous compensators (Statcom).

Due to the multiple-input multiple-output structure of the converter and its various internal dynamics, the control problem of the MMC is intrinsically difficult to address. The vast majority of control methods proposed so far for MMCs is based on hierarchical schemes with multiple single-input single-output (SISO) PI control loops and pulse width modulators (PWM) [5, 6]. However, control schemes with multiple SISO PI control loops tend to perform poorly when fast dynamics during transient operation are required or when operating at low switching frequencies. Therefore, the power electronics community has started to investigate the concept of modern control methods formulated in the time domain, most notably model predictive control (MPC). According to the MPC philosophy, a performance index is minimized subject to the evolution of a dynamical model over a finite-time horizon and constraints on

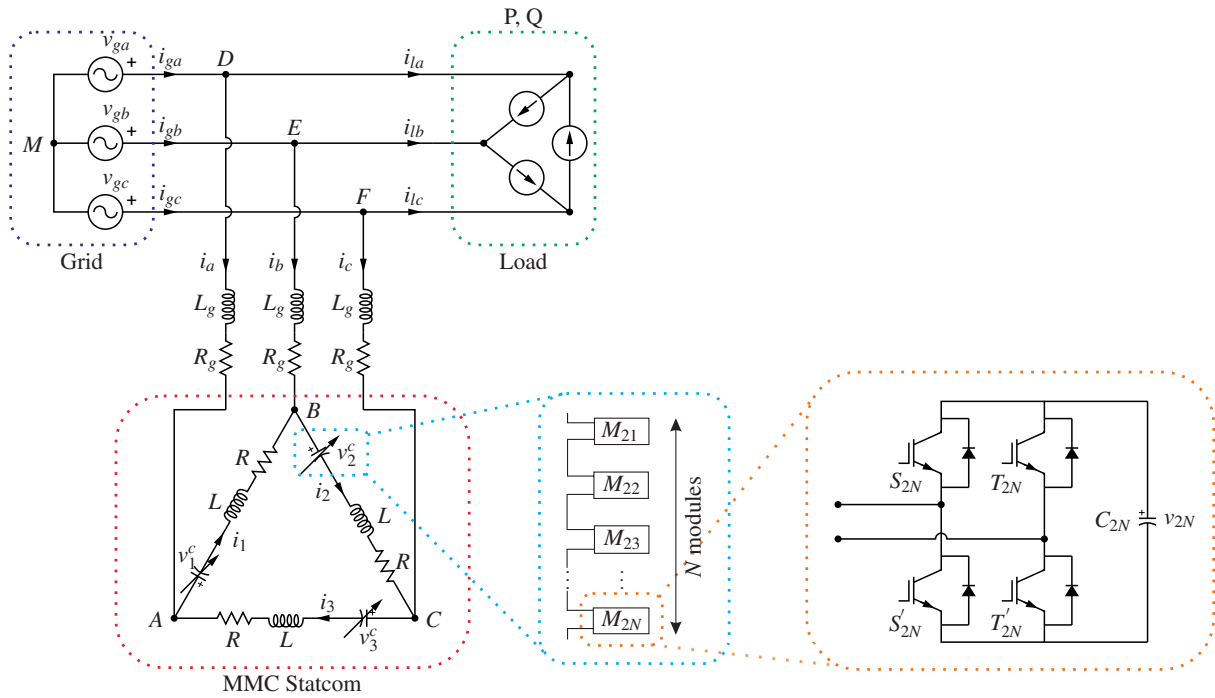


Figure 1: SDBC-MMC Statcom connected to the PCC for reactive power compensation and harmonic filtering of distorted and unbalanced loads

the manipulated variables, states and outputs. The use of a discrete-time state-space model allows MPC to predict the future behavior of the plant and to optimize its control actions accordingly [7].

The literature on MPC schemes for the MMC topology is scarce and mostly restricted to direct MPC methods that do not use a modulator. For example, a direct MPC method with a prediction horizon of length one was proposed in [8] for the single-phase ac-ac MMC topology. A similar method for a back-to-back HVDC system is described in [9]. Both approaches follow the finite control set (FCS) MPC paradigm [10]. Longer prediction horizons were achieved in [11] for a three-phase dc-ac MMC.

This paper proposes an MPC scheme for the SDBC-MMC Statcom. The controller regulates the Statcom currents such that reactive power compensation, load balancing and current harmonic filtering are achieved at the PCC. Moreover, the controller balances the capacitor voltages around their nominal values, while respecting upper and lower limits imposed on them and the branch currents. The control problem is formulated in a hierarchical manner, with MPC constituting the upper layer, which provides the voltage references to the subsequent PWM and balancing control stages.

This paper adopts the modeling concept and control methodology introduced in [12], in which a model predictive current controller for the three-phase dc-ac MMC was proposed. The main contribution of this study is the successful adoption of the above mentioned method to an SDBC-MMC Statcom. To achieve this, the evolution of the load currents is predicted by an extended phase locked loop (EPLL) [13] and a symmetrical component analysis.

2 Modeling

Fig. 1 shows the SDBC-MMC Statcom. Each one of the three branches $r \in \{1, 2, 3\}$ consists of N modules M_{rj} , $j \in \{1, \dots, N\}$ and a branch inductor L . The conduction losses of each branch r are modeled by the resistor R . Each module M_{rj} consists of the four IGBTs S_{rj} , S'_{rj} , T_{rj} and T'_{rj} , which are connected in full-bridge configuration with the capacitor C_{rj} . Its voltage is denoted by v_{rj}^c . The voltages at the module terminals and the branch currents are denoted by v_r^c and i_r , respectively. The switching state of the module M_{rj} is described by the integer variable $s_{rj} \in \{1, 0, -1\}$.

A nonlinear load with active power P and reactive power Q is connected to the PCC. The grid is modeled by the sinusoidal voltage sources v_{gp} , with $p \in \{a, b, c\}$, in series with the grid inductance L_g and the grid resistance R_g . The grid currents, the load currents and the Statcom currents are denoted by i_{gp} , i_{lp} and i_p , respectively. The circulating current i_{cir} that flows through the three branches of the MMC is defined as

$$i_{cir} = (i_1 + i_2 + i_3)/3.$$

For the r th branch we define the insertion index $n_r = \sum_{j=1}^N s_{rj}/N \in \{-1, -\frac{N-1}{N}, \dots, 0, \frac{1}{N}, \dots, 1\}$ as the sum of the switching states normalized by the number of modules per branch. For example, $n_r = 1$ ($n_r = -1$) implies that all N modules in the branch r are at $s_{rj} = 1$ ($s_{rj} = -1$). For a sufficiently large number of modules and/or a high switching frequency, the insertion index n_r can be considered to be a real-valued and bounded variable $n_r \in [-1, 1]$.

Assuming that all modules have the same capacitance $C_m = C_{rj}$ for all r, j , and that the capacitor voltages are balanced [14], the series-connection of the modules inserted into branch r can be described by the branch voltage $v_r^c = n_r v_r^\Sigma$ and the (time-varying) branch capacitance

$$C_r = \frac{1}{n_r} \frac{C_m}{N}. \quad (1)$$

The sum of all capacitor voltages of branch r is defined as $v_r^\Sigma = \sum_{j=1}^N v_{rj}$. Its evolution is governed by the differential equation

$$\frac{dv_r^\Sigma}{dt} = \frac{i_r}{C_r} = \frac{N}{C_m} n_r i_r. \quad (2)$$

Since there are three linearly independent currents, we choose as state variable the branch currents i_r and the sums of the capacitor voltages v_r^Σ of the three branches and define $x = [i_1 \ i_2 \ i_3 \ v_1^\Sigma \ v_2^\Sigma \ v_3^\Sigma]^T$. The grid voltages v_{gp} and the load currents i_{lp} are time-varying affine terms in the nonlinear state-space model. The output of the model are the grid currents i_{gd}, i_{gq} in the rotating dq reference frame, along with the three sums of capacitor voltages per branch v_r^Σ . To this end, we define $y = [i_{gd} \ i_{gq} \ v_1^\Sigma \ v_2^\Sigma \ v_3^\Sigma]^T$.

The state-space equations of the independent branch currents can be easily derived by applying Kirchoff's voltage law to the circuit meshes MDABEM, MDACFM and MDABCFM. The grid currents in the dq frame are computed as

$$\begin{bmatrix} i_{gd} \\ i_{gq} \end{bmatrix} = K(\phi) \left(\begin{bmatrix} 1 & 0 & -1 \\ -1 & 1 & 0 \\ 0 & -1 & 1 \end{bmatrix} \begin{bmatrix} i_1 \\ i_2 \\ i_3 \end{bmatrix} + \begin{bmatrix} i_{la} \\ i_{lb} \\ i_{lc} \end{bmatrix} \right), \quad (3)$$

where $K(\phi)$ denotes the transformation matrix from the three phase abc to the orthogonal dq frame.

The state-space equations describing the dynamical behavior of the MMC contain the nonlinear terms $n_r(t)v_r^\Sigma(t)$ and $n_r(t)i_r(t)$. At time $t = t_0$, a first order Taylor series expansion of the above nonlinear terms around the current operating point of the system, which is given by $n_r(t_0)$, $v_r^\Sigma(t_0)$ and $i_r(t_0)$, is performed. The resulting linearized continuous-time model is discretized using the Euler method with the sampling interval T_s .

3 Model Predictive Control

The hierarchical control scheme is shown in Fig. 2. At the top level, an MPC scheme controls the Statcom currents and the total energy per branch. The cost function over the prediction horizon N_p is defined as

$$J(x(k), u(k-1), U) = \sum_{\ell=k}^{k+N_p-1} \|Q(y^*(\ell) - y(\ell))\|_2^2 + \|R\Delta u(\ell)\|_2^2 + \lambda_\xi \|\xi(\ell)\|_1 + \lambda_\zeta \|\zeta(\ell)\|_1. \quad (4)$$

The matrix Q penalizes the error between the time-varying output reference $y^*(\ell)$ and the output $y(\ell)$. Changes $\Delta u(\ell) = u(\ell) - u(\ell-1)$ in the three (linearized) insertion indices are penalized with the matrix R . Upper and lower soft constraints are imposed on the r th branch current i_r using the slack variable ξ_r , which is aggregated to the vector $\xi = [\xi_1 \ \xi_2 \ \xi_3]^T$. An upper soft constraint is imposed on the sum of capacitor voltages v_r^Σ of the r th branch using the slack variable ζ_r . We define $\xi = [\xi_1 \ \xi_2 \ \xi_3]^T$. The scalar penalties λ_ξ and λ_ζ are chosen as large values.

Two types of constraints are present. The evolution of the linearized and real-valued state-space model of the MMC is described by linear equality constraints. Furthermore, the manipulated variable $u(\ell)$ is bounded by inequality constraints to ensure that the resulting insertion indices are bounded between -1 and 1 .

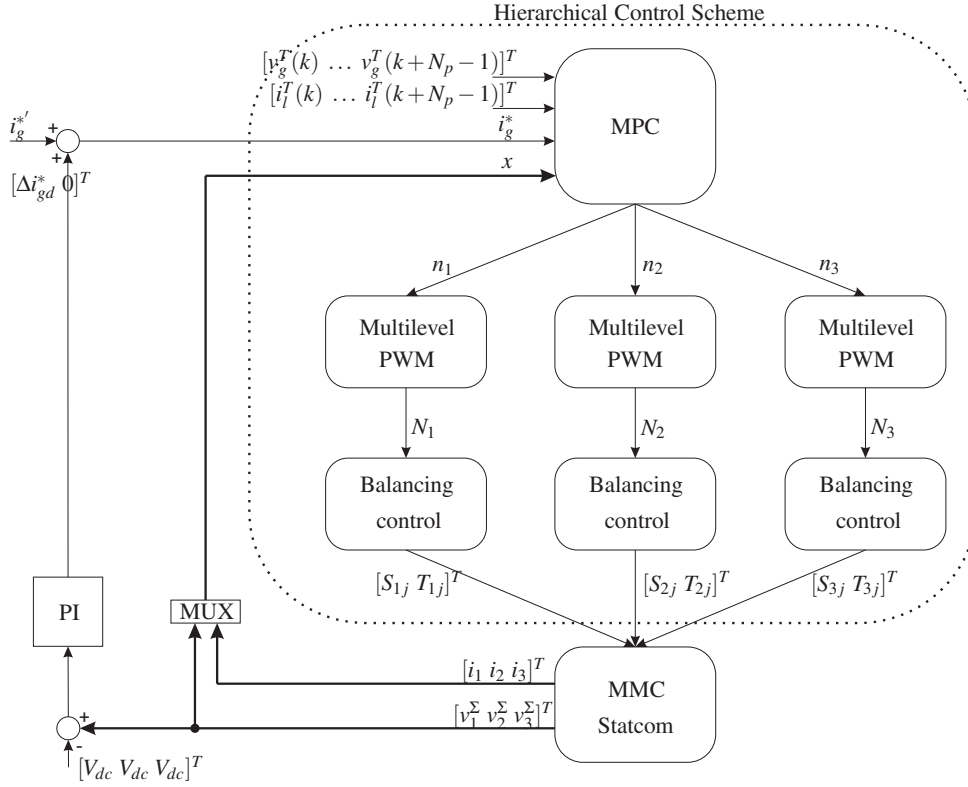


Figure 2: Structure of the proposed control scheme for the SDBC-MMC Statcom

As the cost function (4) is quadratic and the constraints are linear, the optimization problem underlying MPC constitutes a so-called quadratic program (QP). The QP can be formulated and solved efficiently, e.g. by using an active set or an interior point method. The result of the optimization stage is the sequence of optimal control inputs $U = [u^T(k) \ u^T(k+1) \ \dots \ u^T(k+N_p-1)]^T$ at time step k . The first element of the sequence of optimal control inputs is implemented at time-step k and sent to the PWM in the form of the insertion indices n_j . At the next time-step $k+1$, new measurements are obtained and the optimization problem is solved again over a shifted prediction horizon. This so called receding horizon policy provides feedback and ensures that the controller is robust to parameter uncertainties.

MPC requires the evolution of the load current i_l and grid voltage v_g over the prediction horizon. To predict these quantities, a symmetrical component analysis [15, 16] in conjunction with an extended phase locked loop (EPLL) [13] is used. The EPLL estimates the amplitude and angular position of the fundamental component of the input signal s_p at the fundamental frequency f . It also provides the fundamental component phase shifted by 90 degrees. This is denoted by the phase shift operator S_{90} , as shown in Fig. 3.

Consider the unbalanced three-phase system $s = [s_a \ s_b \ s_c]^T$ with the fundamental frequency f . The notion of symmetrical components allows one to decompose s into a set of symmetrical three-phase systems with $s = s^+ + s^- + s^0$, where s^+ , s^- and s^0 denote the positive, negative and zero sequence vectors, respectively. The evolution of the symmetrical components can be easily predicted in the stationary $\alpha\beta$ coordinate system, when assuming constant amplitudes. The positive (negative) sequence vector rotates anticlockwise (clockwise) with the frequency f .

The evolution of an unbalanced three-phase system can be predicted as shown in Fig. 3. To address unbalanced three-phase systems with harmonic distortions, the scheme shown in Fig. 3 can be extended by a sequential implementation of the EPLL and symmetrical component decomposition entities. When considering the fundamental component and the third and fifth harmonics, for example, the scheme in Fig. 3 is repeated three times and run at the frequencies $f \in \{50, 150, 250\}$. The EPLL at $f = 150$ is fed by the difference between the input and output signals of the first EPLL, which operates at $f_0 = 50$.

The aforementioned method predicts the evolution of the grid voltages $[v_g^T(k+1) \ \dots \ v_g^T(k+N_p-1)]^T$ and load currents $[i_l^T(k+1) \ \dots \ i_l^T(k+N_p-1)]^T$ over the prediction horizon N_p . These vectors are provided as inputs to the MPC scheme, as depicted in Fig. 2.

At the middle level of the hierarchical control scheme, the insertion indices are translated into the three

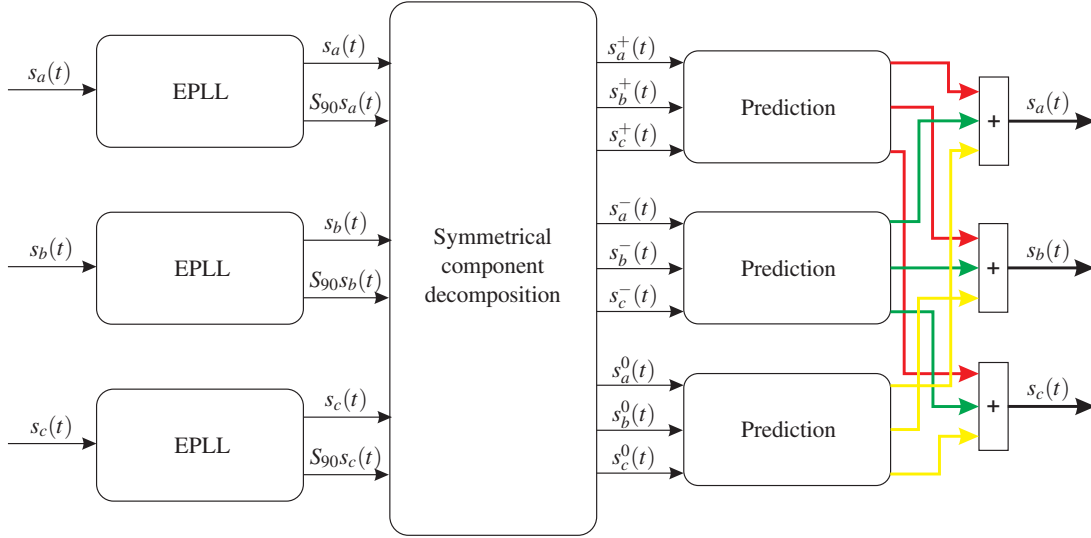


Figure 3: Prediction of the evolution of an unbalanced three-phase quantity

integer variables $N_r \in \{-N, -N+1, \dots, N\}$, which denote the number of modules to be inserted per branch. A carrier-based multilevel PWM is used for this task, as described in [17]. At the lower layer, each branch uses an independently operating controller that utilizes the redundancy within that branch to balance the capacitor voltages, by selecting the gating commands for the individual modules. The balancing controller operates on the basis of keeping two separate and mutually exclusive lists, namely "List ON" and "List OFF", according to the current state of the modules in the branch. In each of the two lists, the capacitor voltages are sorted in an ascending or descending order of their voltage values depending on the polarity of the respective branch current. "List ON" is always prioritized and only if all the modules of that list have been selected then a module of the "List OFF" is selected and turned on. In case that the "List ON" contains more modules than required, the remaining modules are turned off. The complete control scheme is summarized in Fig. 2, in which i_g^* denotes the reference of the dq grid current. The q -component is usually set to zero, while the d -component depends on the active power P that is consumed by the load. P can be calculated analytically using the fundamental component of the load current, which is provided by the EPLL. A PI controller is added that compensates for the energy losses in the MMC, by monitoring the deviation of the total capacitor energy from its reference and by adding an appropriate correction signal Δi_{gd}^* to the d -component of the grid current reference.

4 Performance Evaluation

To demonstrate the performance of the proposed MPC scheme, consider an SDBC-MMC Statcom with $N = 8$ modules per branch. A regularly sampled multilevel carrier-based PWM with phase disposition is used with a carrier frequency of 2.5 kHz. The different triangular carriers are not interleaved. The gains of the loss compensating PI controller are set to $K_p = 1$ and $K_i = 0.1$ for the proportional and integral terms. This ensures a slow and smooth compensation of the energy losses.

Parameter	Symbol	pu value	SI value
Grid frequency	f_0	1	50 Hz
Reference voltage for v_r^Σ	V_{dc}	2.2268	20 kV
Nominal grid line-to-line voltage	V_g	1.2247	11 kV
Rated load current	I_l	0.7071	2.08 kA
Module capacitance	C_m	9.5922	10 mF
Branch resistance	R	0.0066	20 m Ω
Grid resistance	R_g	0.0067	20.4 m Ω
Branch inductance	L	0.1	0.972 mH
Grid inductance	L_g	0.1	0.972 mH

Table I: System parameters

The MPC scheme is executed at the peaks and valleys of the triangular carrier, i.e. every $200\mu\text{s}$. The state vector x is assumed to be available to the controller along with the time-varying reference signal y^* . Measurement and computational delays are assumed to be fully compensated. The computed insertion indices are kept constant between time steps k and $k+1$ and sent to the multilevel PWM stage. For the objective function, the penalties

$$Q = \begin{bmatrix} \begin{bmatrix} 1 & 0 \\ 0 & 10 \end{bmatrix} & \mathbf{0}_{2 \times 3} \\ \mathbf{0}_{3 \times 2} & \mathbb{I}_{3 \times 3} \end{bmatrix}, \quad R = \mathbb{I}_{3 \times 3}, \quad \lambda_\xi = 10^5, \quad \lambda_\zeta = 10^5$$

are chosen. The soft constraints are activated at $\underline{i} = -1.1\text{ pu}$, $\bar{i} = 1.1\text{ pu}$ and $\bar{v} = 1.1V_{\text{dc}}$. The prediction horizon is set to $N_p = 6$. The MMC Statcom, MPC scheme, PWM and balancing controller were implemented in Matlab/Simulink and PLECS. To formulate and solve the QP problem, the Multi-Parametric Toolbox 3.0 [18] and the Gurobi solver [19] were used.

4.1 Steady-State Operation with Load Distortions

Consider a nonlinear load that consumes on average the real power $P = 0.8\text{ pu}$ and the reactive power $Q = 0.6\text{ pu}$. The load draws a current of magnitude 1 pu with a 5th harmonic of amplitude 0.2 pu and a 19th harmonic of amplitude 0.05 pu . The MMC Statcom compensates for the mean reactive power and the load current harmonics, as it is shown in Fig. 4.

The compensation of the load current harmonics is verified in Fig. 5, which shows the harmonic content of the load, Statcom and grid currents. The 5th harmonic at 250 Hz and the 19th harmonic at 950 Hz in the load current are eliminated in the grid current. Moreover, the fundamental component of the load current is at the rated value of 1 pu , while the fundamental component of the grid current is at 0.8 pu , since the grid is required to deliver only real power to the load. The fundamental component of the Statcom current is 0.6 pu so as to compensate for the load's reactive power.

Over a time window of 200 ms , the mean square error (MSE) of the grid current tracking error, the THD of the grid currents and the device switching frequency are evaluated. The MSE is $23 \cdot 10^{-5}\text{ pu}$, the THD of the grid currents is 1.01% , while the average device switching frequency is 495 Hz .

The branch currents are shown in Fig. 6(a), while Fig. 6(b) shows the circulating current, which is relatively small. The operation of the balancing algorithm can be observed in Fig. 6(c), which shows the capacitor voltage waveforms. These voltages remain balanced within $\pm 4\%$ of their nominal value. The visible differences in the capacitor voltages are due to the low switching frequency. The soft constraints on the capacitor voltages and branch currents are inactive during steady-state operation.

4.2 Operation during Load Transients

Next, the dynamic behavior of the SDBC-MMC Statcom is investigated using the following (somewhat hypothetical) experiment. Initially, the load draws the reactive power $Q = 1\text{ pu}$, which is fully compensated for by the Statcom. At time $t = 56\text{ ms}$, the load is disconnected, whereas at $t = 84\text{ ms}$ it is reconnected. The response of the MMC Statcom to these load steps is shown in Fig. 7. The grid currents remain close to zero, and the disturbance of disconnecting and reconnecting the reactive load to the grid is rapidly rejected.

Specifically, when inspecting Fig. 7, it can be seen that during both the negative and the positive load steps, the Statcom currents require only $400\mu\text{s}$ (i.e. two control cycles) to settle at their new reference values. These fast current responses are achieved by the MPC scheme without overshoots. Despite these fast transients, the safety constraints are respected. This can be appreciated by inspecting Fig. 8(a), which depicts the branch currents during the transients. Similarly, the capacitor voltages of the modules remain close to their nominal values, as exemplified in Fig. 8(c) for the first branch. This is a significant achievement by the controller, since the second-order energy exchange between the branch inductors and the module capacitors must be taken into account by the controller to avoid overshoots in the capacitor voltages and branch currents. As shown in Fig. 8(d), the controller issues abrupt control actions during the transients to achieve as fast a current response as possible. It can be seen that the MPC scheme fully utilizes the available branch voltages by inserting the maximal number of modules available per branch when required. During steady-state operation, however, smooth control actions prevail and the modules are added and removed from the branches accordingly, as can be seen in Fig. 6(d).

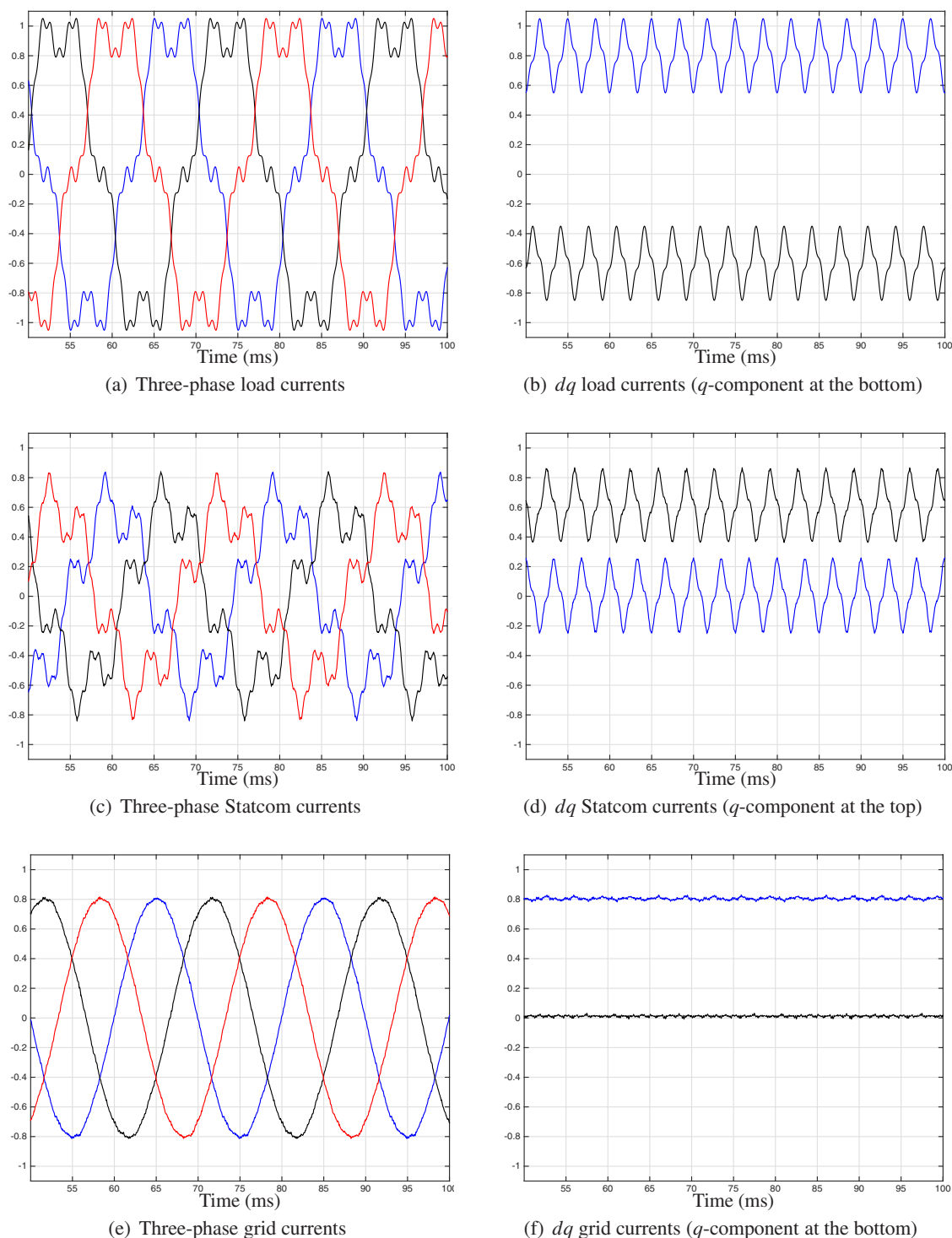


Figure 4: Three-phase and dq currents of the load, Statcom and grid during steady-state operation

5 Conclusion

A model predictive current control scheme with a PWM was proposed in this paper for the MMC in delta configuration acting as a Statcom. Due to its ability to address the MMC as a multiple-input multiple-output (MIMO) system with operating and safety constraints, MPC outperforms most of the existing control approaches for the MMC, particularly during transients. Very fast current responses close to the physical limits of the MMC are achieved. Overshoots in the capacitor voltages and the branch currents are avoided, and the operation of the converter within safe operating limits is ensured under all circumstances thanks to the soft constraints added to the cost function. At steady-state operation,

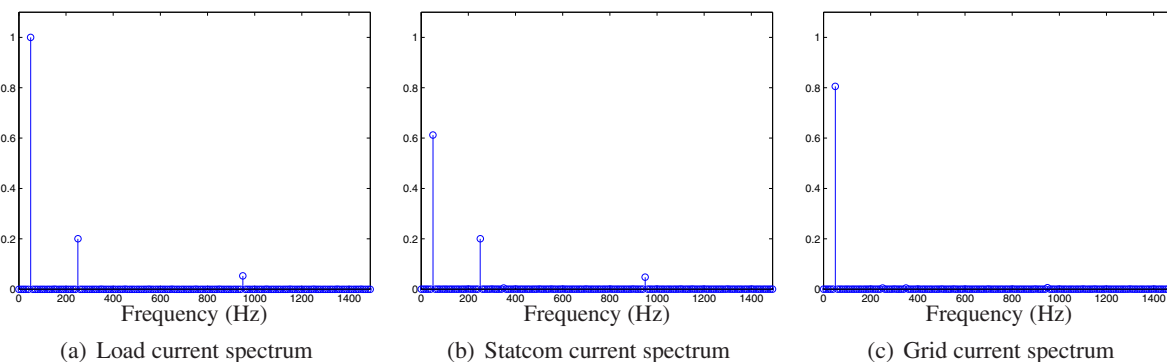


Figure 5: Harmonic spectra of the load, Statcom and grid currents during steady-state operation

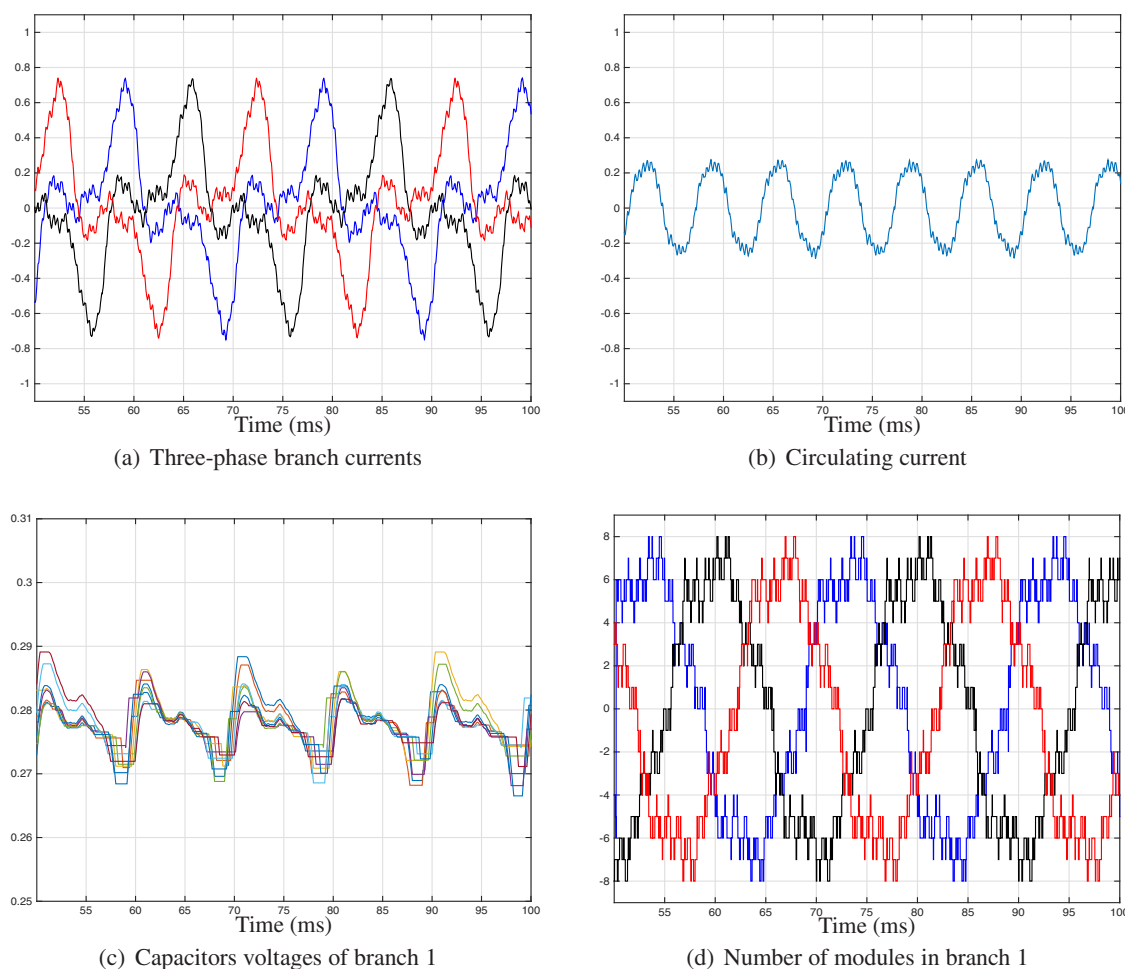


Figure 6: Branch currents, circulating current, capacitor voltages and number of modules during steady-state operation

it was shown that in the presence of a distorted load a low current THD of about 1% can be achieved, while operating the IGBTs at a switching frequency of less than 500 Hz. During load transients, current responses with settling times of less than 0.5 ms can be achieved for a grid inductance of 0.1 pu.

References

[1] H. M. Pirouz and M. T. Bina. New transformerless STATCOM topology for compensating unbalanced medium-voltage loads. In *Proc. Eur. Conf. on Power Electron. and Applicat.*, pages 1–9, 2009.

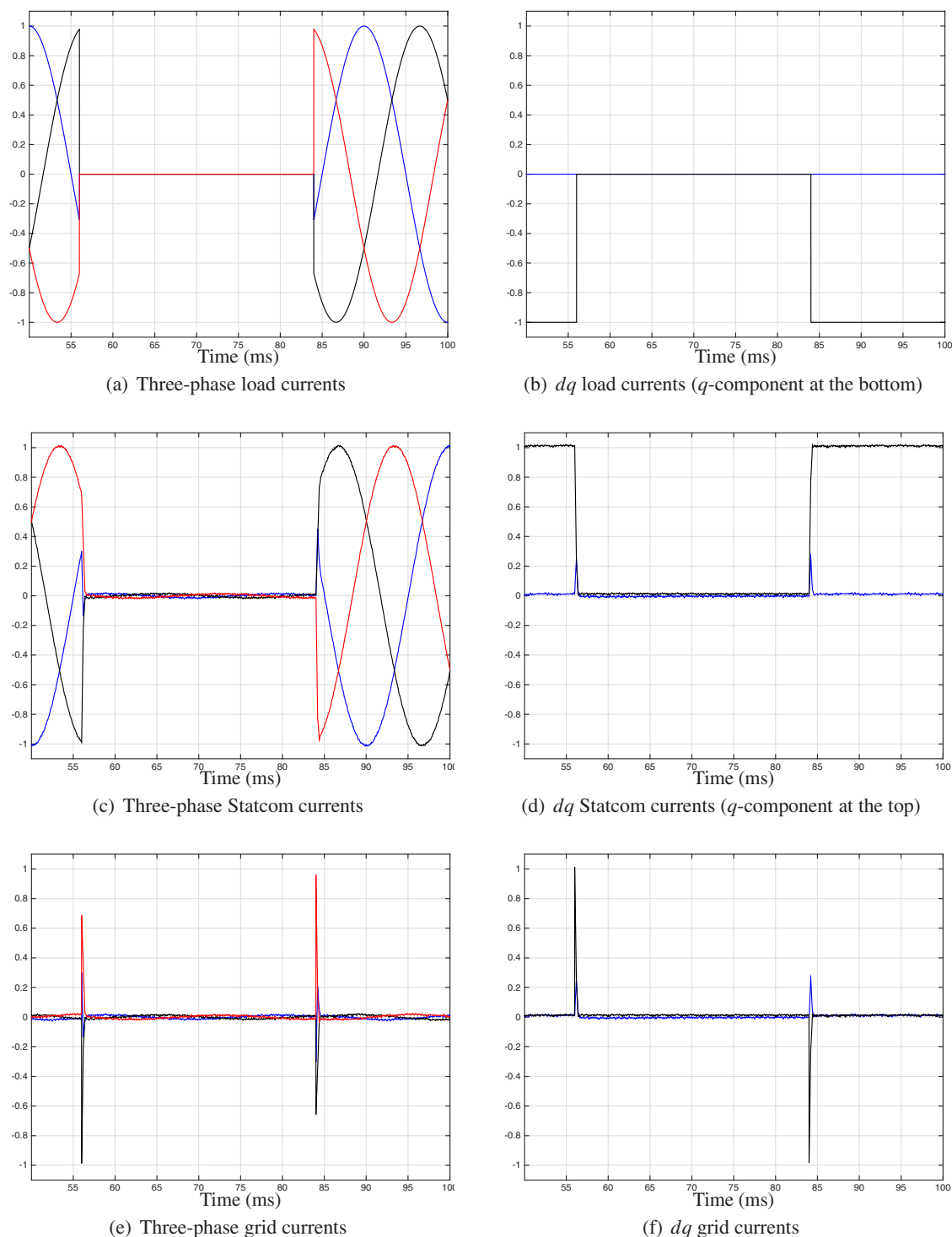


Figure 7: Three-phase currents of the load, Statcom and grid during reactive power steps of the load

- [2] H. Akagi. Classification, terminology, and application of the modular multilevel cascade converter (MMCC). *IEEE Trans. Power Electron.*, 26(11):3119–3130, Nov. 2011.
- [3] H. P. Mohammadi and M. T. Bina. A transformerless medium-voltage STATCOM topology based on extended modular multilevel converters. *IEEE Trans. Power Electron.*, 26(5):1534–1545, 2011.
- [4] A. Lesnicar and R. Marquardt. An innovative modular multilevel converter topology suitable for a wide power range. In *Proc. IEEE Power Tech. Conf.*, Bologna, Italy, Jun. 2003.
- [5] A. Antonopoulos, L. Angquist, and H. P. Nee. On dynamics and voltage control of the modular multilevel converter. In *Proc. Eur. Conf. on Power Electron. and Applicat.*, 2009.
- [6] M. Hagiwara and H. Akagi. Control and experiment of pulsewidth-modulated modular multilevel converters. *IEEE Trans. Power Electron.*, 24(7):1737–1746, Jul. 2009.

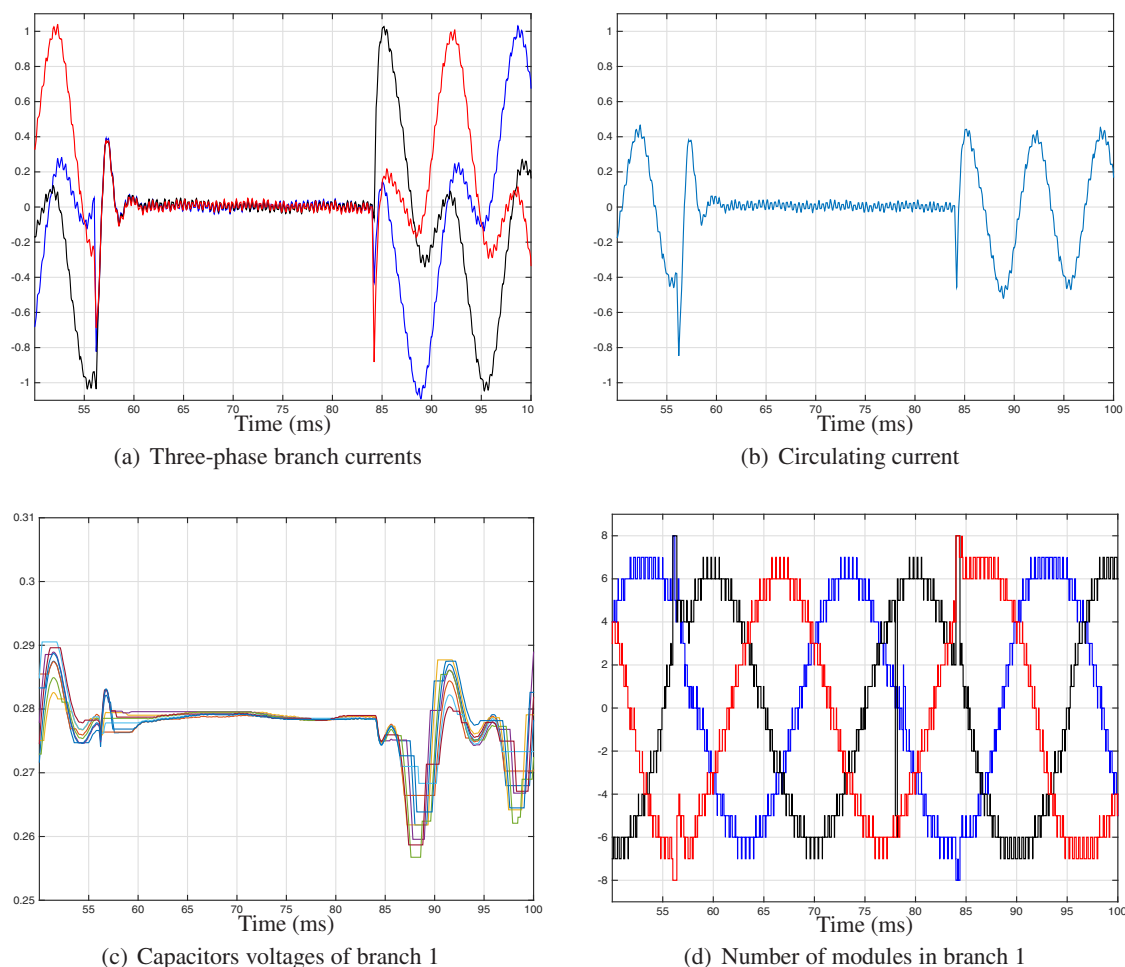


Figure 8: Branch currents, circulating current, capacitor voltages and number of modules during load power steps

- [7] J. B. Rawlings and D. Q. Mayne. *Model predictive control: Theory and design*. Nob Hill Publ., Madison, WI, USA, 2009.
- [8] M. A. Pérez, J. Rodríguez, E. J. Fuentes, and F. Kammerer. Predictive control of AC-AC modular multilevel converters. *IEEE Trans. Ind. Electron.*, 59(7):2832–2839, Jul. 2012.
- [9] J. Qin and M. Saeedifard. Predictive control of a modular multilevel converter for a back-to-back HVDC system. *IEEE Trans. Power Deliv.*, 27(3):1538–1547, Jul. 2012.
- [10] P. Cortés, M. P. Kazmierkowski, R. M. Kennel, D. E. Quevedo, and J. Rodríguez. Predictive control in power electronics and drives. *IEEE Trans. Ind. Electron.*, 55(12):4312–4324, Dec. 2008.
- [11] B. S. Riar, T. Geyer, and U. K. Madawala. Model predictive direct current control of modular multilevel converters: Modelling, analysis, and experimental evaluation. *IEEE Trans. Power Electron.*, 30(1):431–439, Jan. 2015.
- [12] G. Darivianakis, T. Geyer, and W. van der Merwe. Model predictive current control of modular multilevel converters. In *Proc. IEEE Energy Convers. Congr. Expo.*, pages 5016–5023, 2014.
- [13] M. R. Iravani and M. Karimi-Ghartemani. Online estimation of steady state and instantaneous symmetrical components. *Proc. IEE Gener., Transm. and Distr.*, 150(5):616–622, 2003.
- [14] K. Ilves, A. Antonopoulos, S. Norrga, and H. P. Nee. Steady-state analysis of interaction between harmonic components of arm and line quantities of modular multilevel converters. *IEEE Trans. Power Electron.*, 27(1):57–68, 2012.
- [15] G. C. Paap. Symmetrical components in the time domain and their application to power network calculations. *IEEE Trans. Power Syst.*, 15(2):522–528, 2000.
- [16] H. Akagi, Y. Kanazawa, and A. Nabae. Instantaneous reactive power compensators comprising switching devices without energy storage components. *IEEE Trans. Ind. Appl.*, IA-20(3):625–630, 1984.
- [17] G. Carrara, S. Gardella, M. Marchesoni, R. Salutati, and G. Sciuotto. A new multilevel PWM method: a theoretical analysis. *IEEE Trans. Power Electron.*, 7(3):497–505, Jul. 1992.
- [18] M. Herceg, M. Kvasnica, C. N. Jones, and M. Morari. Multi-parametric toolbox 3.0. In *Proc. Eur. Control Conf.*, pages 502–510, Zürich, Switzerland, July 17–19 2013.
- [19] Gurobi Optimization, Inc. Gurobi optimizer reference manual, 2014. <http://www.gurobi.com>.